

Original Article

Brainstem injury associated with supratentorial lesions is revealed by electronystagmography of the cold caloric reflex test

Qizhi Fu¹, Zhiguo Qi², Ruirui Yang³, Ke Cheng⁴, Yongtao Yang⁴, Peng Xie⁵

¹Department of Neurology, The First Affiliated Hospital and College of Clinical Medicine of Henan University of Science and Technology, Luoyang, China; ²Department of Neurology, The First Affiliated Hospital of Jiamusi University, Jiamusi, China; ³Department of Neurology, The Shandong Provincial Hospital, Jinan, China; ⁴Institute of Neuroscience, Chongqing Medical University, Chongqing, China; ⁵Department of Neurology, The First Affiliated Hospital of Chongqing Medical University, Chongqing, China

Received December 20, 2016; Accepted March 22, 2017; Epub May 15, 2017; Published May 30, 2017

Abstract: To explore the brainstem injury associated with supratentorial lesions, we conducted analysis of ICP levels and detected ENG parameters by using the cold caloric reflex test and histopathological examinations of the brainstem. Rat model of intracerebral hemorrhage was well-established in the study of supratentorial lesions of varying severities (n=210). Intracerebral pressure monitoring and electronystagmography of the cold caloric reflex test were simultaneously performed in animals. Apoptotic, immunohistochemical, and histopathological changes in different segments of the brainstem were investigated at various time intervals. Electronystagmography parameters were analyzed by cold caloric reflex test. The result showed that the increase of intracerebral pressure was correlated with lesion severity including elevating levels and rostral-caudal progression of neuronal apoptosis, demyelination, N-methyl-D-aspartate cell receptor down-regulation ($r=0.815$), and histopathological changes. Multiple discrimination analysis of electronystagmography parameters presented a diagnostic accuracy rate of 79.5% in localizing brainstem injury. In conclusion, our data demonstrated that electronystagmography monitoring along with the cold caloric reflex test performed a favorable effect on the estimation of brainstem injury in ICH rat model, which provided a potential bedside diagnostic tool to assess and predict the progress of supratentorial lesion patient in future.

Keywords: Brainstem injury, electronystagmography, cold caloric reflex

Introduction

Brainstem displacement associated with supratentorial lesions is an important factor of neurological deterioration in spite of transtentorial herniation status [1]. Howell [2] proposed in 1961 that supratentorial lesions produced cerebral edema that elevated intracerebral pressure (ICP). The ICP elevation was thus suggested to result in brainstem displacement and subsequent brainstem injury. Wijdicks and Miller [3] later reported mid brain displacement and an abnormally high signal from the thalamus to the upper pons were found based on T2-weighted MRI images of patients with supratentorial intracerebral hemorrhage (ICH). These combined findings suggested that the rise of ICP led to brainstem shift that caused direct

traumatic injury or secondary injury to the brainstem via ischemia and/or hemorrhage [4, 5].

Presently, Rosenberg's ICH model is well developed for the study of through the establishment of acute supratentorial hemorrhagic lesions in the rat basal ganglia and anomalies were observed in the vestibulo-ocular reflex (VOR), which was significant in the pathway through the midbrain and pontine segments of the brainstem [6, 7].

It has been demonstrated that changes in the VOR were studied by using cold caloric reflex test, a bedside physical examination technique, in response to ice water irrigation of the external auditory meatus [8-10]. In addition, electronystagmography (ENG) was applied, along with

Brainstem injury of cold caloric reflex test

the cold caloric reflex test, in the objective measurement of the VOR [11-17]. Recent studies on quantification of VOR reactions (e.g., dysrhythmia, hyporeflexia, and areflexia) exhibited an effective evaluation way to rate and localize brainstem injuries [18]. Also, several studies showed that VOR hyporeflexia in conjunction with the cold caloric reflex test was extended to utilize in the clinical setting of the increase of ICP such as supratentorial hemorrhagic lesions, tumors, and benign intracranial hypertension syndrome [19, 20].

The anatomic loop of the VOR crossed over the brainstem including ocular motor nucleus, vestibular nucleus, abducens nucleus and medial longitudinal fasciculus. The cold caloric test effectively detected the damage of one or some links of the loop. The examination through a rigorous analysis of changes in the VOR and ICP levels provides a potential tool to estimate the degree of brainstem injury in the setting of supratentorial lesions. Our study thus aims to observe supratentorial lesions and detect ICP, ENG via the cold caloric reflex test and histopathological examinations of the brainstem, in order to lay the foundation for the development of new bedside method in monitoring and predicting the progress of supratentorial lesions.

Materials and methods

Rosenberg's ICH model

An experimental ICH model was established in accordance with Rosenberg [7]. Adult male Sprague-Dawley rats (n=210) weighing 300-350 g were anesthetized with 10% chloralhydrate (400 mg/kg, i.p.). After each rat was fixed in a stereotaxic frame (Narishige Co., Japan), a burr hole (diameter: 1.0 mm) was drilled in the right skull (coordinates: 0.2 mm anterior, 5.8 mm ventral, and 3.0 mm lateral to the bregma).

The ICH models (n=144) were divided into three subgroups: the 0.3 U ICH group (n=48), 0.6 U ICH group (n=48), and 0.9 U ICH group (n=48). Five- μ L micropipettors (AnTingMicropipettor Factory, Shanghai, China) filled with 2 μ L saline containing 0.3 U, 0.6 U, or 0.9 U of bacterial collagenase type VII (Sigma, St. Louis, MI, USA) were then inserted into the right striatum for a 5 min infusion. The needle was left in for 10 min post-injection and then withdrawn. Each

ICH subgroup was then randomly divided into six time interval subgroups (12 h, 24 h, 48 h, 72 h, 5 d, and 7 d; n=8 for each time interval in each ICH subgroup).

The saline control group (n=48) was established delivering the equivalent volume of saline by intrastriatal injection. The sham control group (n=18) was established without infusion. Body temperature was maintained at 37°C with a feedback-controlled heating pad (Chengdu Instrument Factory, China) and monitored with a rectal probe. All subjects were placed in boxes and given free access to food and water. All surgical procedures and post-operative care were performed in accordance with the guidelines of the China Zoological Society. The protocols in this study were approved by the Ethics Committee of The first affiliated hospital of Henan science and technology university. Animal testing was performed in accordance with the international guiding principles for biomedical research.

ENG recording of the cold caloric reflex test

ENG recording of the cold caloric reflex test was performed at 12 h, 24 h, 48 h, 72 h, 5 d, and 7 d post-injection. Each rat was restrained in a prone position within a home-made bin; the angle between the coronal and horizontal planes was fixed at 42° in order to position the horizontal semicircular canal perpendicular to the horizontal plane. Two pairs of silk-silver electrodes (platinum, diameter: 200 μ m) were attached to the angulus oculi lateralis and angulus oculi nasalis of both eyes [21, 22], and a reference electrode was attached to the forehead vertex at the midline. The positive electrodes were placed in the angulus oculi nasalis of the left eye and the angulus oculi nasalis of the right eye, this resulted in a positive wave recorded by the instrument when eyeballs move toward the right. Conversely, the negative electrodes were placed in the angulus oculi nasalis of the right eye and the angulus oculi nasalis of the left eye that resulted a negative wave recorded by the instrument when the eyeball move towards the left ([Supplementary Figure 1](#)). Hence, the waves were recorded as microvolt (μ V) instead of degree (eye position). The five electrode wires were connected with the two channels of RM6240C multichannel polygraph recorder (Chengdu Instrument Co., China) respectively for ENG recordings. The

Brainstem injury of cold caloric reflex test

Table 1. The coordinate positions of nuclei in the rat brainstem

	Coordinate Position (mm)			Point of Maximum Area (mm)			
	Post quadrigeminal bodies	Post bregma	Lateral to midline	Post quadrigeminal bodies	Post bregma	Lateral to midline	Depth to cupule
OMN	3.10-3.75	6.24-6.96	0.05-0.30	3.50	6.72	0.15	6.50
PPRN	1.60-3.20	7.08-8.88	0.50-2.10	2.40	8.52	1.50	8.70
VN	3.30-4.50	9.72-12.48	1.00-2.80	3.60	10.92	1.40	7.80

recording parameters of RM6240C multichannel polygraph recorder were set as sampling frequency 800 Hz, time constant 5.0 s and the filter (3-30) Hz. ENG system were calibrated by ensured that the recorder showed a stable potential line at $0 \pm 0.25 \mu\text{V}$ for 30 s that represented the eye position in horizontal central before the irrigation of cold water.

For the cold caloric reflex test, the auditory canal was steadily irrigated at a rate of 1 ml/s using an infusion pump with 50 ml of cold water (0°C) for 50 s. Both ears were verified as normal before initiating the test. Eye-movements were simultaneously observed. The cold caloric reflex test induced horizontal nystagmus (the physiologically normal response) in both control groups. Each ENG recording session lasted 20 min following initiation of the cold caloric reflex test. The calibration was to modulate ENG parameters, namely latency (Lat), frequency (Freq), amplitude (Amp), slow-phase velocity (SPV) and circadian variation index (CVI), were calculated from recorded nystagmus curves, as previously described [23]. Lat was defined as the time interval from the start of cold caloric reflex irrigation to the appearance of continuous nystagmus (defined as >5 sequential waves of identical frequency and amplitude with each constituent wave demonstrating both slow and fast phases) ([Supplementary Figure 2](#)). SPV was defined as the Amp divided by the duration of the slow-phase ($\mu\text{V/s}$). CVI was defined as the number of abnormal frequency waveforms divided by the total number of waveforms. Freq, Amp, SPV and CVI were calculated through analyzing the middle-segment of the nystagmus curve after divided the curve into three segments. If no nystagmus response occurred following administration of the cold caloric reflex test, the animal was re-subjected to the test after a 5-min intermission to confirm the absence of the reflex.

Both horizontal and vertical nystagmi were observed in both control groups. A bounce-like

horizontal nystagmus, in which the fast-phase moved contra laterally to the irrigated ear, and was considered to be the primary nystagmus.

ICP monitoring

ICP monitoring was performed simultaneously with nystagmus recording using a RM6240C multi-channel polygraph recorder (Chengdu Instrument Factory, China). The head of each rat was positioned in a stereotactic guide apparatus. A cannulation hole was made with a dental drill (coordinates: 0.5 mm posterior to bregma, 1.0 mm lateral to the midline and 4.0 mm below the skull). A 10G lateral ventricular cannula (Plastics One, Chengdu Instrument Factory, China) was vertically inserted into the brain parenchyma. The other end of the cannula was connected to a pressure transducer. The pressure transducer recording showed a curve that harmonized with the breathing cycle, verifying a successful intraventricular cannulation. After this verification, the catheter was then cemented in place.

Brainstem sectioning & HE staining

At 12 h, 24 h, 48 h, 72 h, 5 d, and 7 d post-injection, rats were sacrificed by an overdose of 10% chloralhydrate. Their hearts were perfused with 200 mL ice-cold saline, followed by 200 mL of 4% paraformaldehyde (pH 7.5). The whole brain was then surgically removed. The brainstems were separated from the forebrains and stored overnight in fixation fluid. After fixation, the brainstems were dehydrated in ascending ethanol concentrations up to 95% and then embedded in paraffin. Fixed brainstems were coronally sectioned into four segments proceeding dorsally to ventrally, namely the dorsal midbrain (corpora quadrigemina), the ventral midbrain (midbrain tegmentum), the dorsal pons (pontine tegmentum), and the ventral pons. Four- μm sections were then prepared from these four segments. Two slices of each segment were stained with hematoxylin & eosin (HE) to assess histopathological changes.

Brainstem injury of cold caloric reflex test

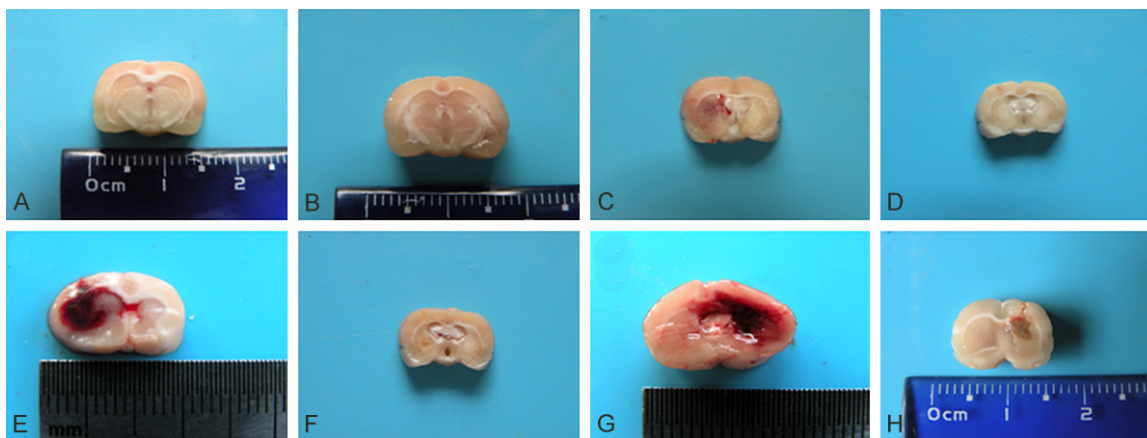


Figure 1. Coronal sections of basal ganglia from controls and ICH rats induced by various dosages of collagenase VII. (A) The sham control group at 72 h, (B) the saline control group at 72 h, (C, D) the 0.3 U ICH group at 72 h and 7 d, (E, F) the 0.6 U ICH group at 72 h and 7 d, and (G, H) the 0.9 U ICH group at 72 h and 7 d. The hematoma enlarged post-injection and peaked at 72 h with midline drift, and then was absorbed after 5 d. There was a positive relationship between the collagenase dose and hematoma volume (C, E, G).

Immunohistochemistry

According to Paxinos and Watson [24], the brainstems were sectioned in either the coronal, sagittal or horizontal planes. The mid-brain's ocular motor nucleus (OMN), the upper pons' paramedian pontine reticular nucleus (PPRN), and the lower pons' vestibular nucleus (VN) were identified; their coordinate positions and points of maximum area were presented in **Table 1**. Eight sections of OMN from each subject were analyzed using antibodies against N-methyl-d-aspartate receptor 1 (NMDAR1) and GABA A receptor $\alpha 1$ (GABA-AR $\alpha 1$). Four sections of the medial longitudinal fasciculus (MLF; a structure that runs through the mid-brain, upper pons and lower pons) from each subject were analyzed using antibodies against myelin basic protein (MBP).

Briefly, all sections were rinsed 10 min thrice in KPBS, blocked for endogenous peroxidase activity for 15 min using 3% H₂O₂ in KPBS, rinsed again for 10 min thrice in KPBS, and incubated for an additional 20 min in a solution containing 5% goat serum, 1.0% bovine serum albumin (BSA) and 0.3% Triton X-100 (TX) in KPBS. Sections were then rinsed for 10 min thrice in KPBS before incubation overnight at 4°C with primary rabbit anti-NMDAR1 (bs-1068R, Bios Co., Beijing, China), anti-GABA-AR $\alpha 1$ (bs-1232R, Bios Co., Beijing, China), and anti-MBP (Bios Co., Beijing, China), all diluted 1:200 in KPBS with 0.3% TX and 1% BSA. The next day, all sections were rinsed 10 min thrice

in KPBS containing 0.1% TX and incubated for 60 min at room temperature in a biotinylated goat anti-rabbit antibody (Beyotime Co., China) diluted 1:200 in KPBS-T. Sections were then rinsed 10 min thrice in KPBS-T, incubated for 60 min in ABC streptavidin horseradish peroxidase (ZSGB-BIO Co., China), rinsed 10 min thrice in KPBS and finally reacted for peroxidase activity using DAB as a chromogen (0.04% diaminobenzidine tetrahydrochloride and 0.03% H₂O₂ in Tris-HCl buffer). Sections were stained with hematoxylin, washed for 10 min thrice in deionized water, and then mounted on slides with Permount.

Images were captured using a Nikon Eclipse E100 microscope equipped with a Nikon Intensilight C-HGFI (Nikon, Tokyo, Japan). Expression levels of NMDAR1, GABA-AR $\alpha 1$ and MBP were measured by average optical density (AOD) calculated using a computerized image analysis system (Image-Pro Plus 6.0). The AOD of NMDAR1 and GABA-AR $\alpha 1$ was measured from 0.1-mm² stained sections of the mid-brain's OMN. The AOD of MBP was measured in 0.1-mm² stained sections of MLF from the mid-brain, upper pons and lower pons.

TUNEL assay

Four adjacent sections were selected from the midbrain's OMN, the upper pons' PPRN and the lower pons' VN of each rat across all time intervals (12 h, 24 h, 48 h, 72 h, 5 d and 7 d) for terminal deoxynucleotidyl transferase UTP

Brainstem injury of cold caloric reflex test

Table 2. Qualitative overview of comparative significant changes in Rosenberg's ICH model†

Group	ENG parameters						NMDAR1	Apoptosis			MBP		HE			
	ICP	Lat	Freq	Amp	SPV	CVI	MB(OMN)	MB	UP	LP	MB	UP	LP	MB	UP	LP
Sham control																
Saline control																
0.3 U (12 h)		↑*					↓	↑								
0.3 U (24 h)	↑	↑	↓	↓	↓	↑	↓	↑								
0.3 U (48 h)	↑	↑	↓	↓	↓	↑	↓	↑	↑					↑		
0.3 U (72 h)	↑	↑	↓	↓	↓	↑	↓	↑	↑		↓			↑		
0.3 U (5 d)		↑	↓	↓	↓	↑	↓	↑	↑		↓			↑		
0.3 U (7 d)							↓	↑	↑		↓			↑		
0.6 U (12 h)	↑	↑↑	↓	↓	↓	↑	↓↓	↑↑								
0.6 U (24 h)	↑↑	↑↑	↓↓	↓↓	↓↓	↑↑	↓↓	↑↑			↓			↑	↑	
0.6 U (48 h)	↑↑	↑↑	↓↓	↓↓	↓↓	↑↑	↓↓	↑↑	↑	↑	↓			↑↑	↑	
0.6 U (72 h)	↑↑	↑↑	↓↓	↓↓	↓↓	↑↑	↓↓	↑↑	↑↑	↑	↓↓	↓↓		↑↑	↑	
0.6 U (5 d)	↑	↑↑	↓↓	↓↓	↓↓	↑↑	↓↓	↑↑	↑↑	↑	↓↓	↓↓		↑↑	↑	
0.6 U (7 d)	↑	↑	↓	↓	↓	↑	↓↓	↑↑	↑↑	↑	↓↓	↓↓		↑↑	↑	
0.9 U (12 h)	↑↑	↑↑↑	↓↓	↓↓	↓↓	↑↑	↓↓↓	↑↑↑			↓			↑	↑	↑
0.9 U (24 h)	↑↑↑	↑↑↑	↓↓↓	↓↓↓	↓↓↓	↑↑↑	↓↓↓	↑↑↑			↓			↑↑	↑↑	↑
0.9 U (48 h)	↑↑↑	↑↑↑	↓↓↓	↓↓↓	↓↓↓	↑↑↑	↓↓↓	↑↑↑	↑↑↑	↑↑	↓↓	↓	↓	↑↑↑	↑↑	↑
0.9 U (72 h)	↑↑↑	-	-	-	-	-	↓↓↓	↑↑↑	↑↑↑	↑↑	↓↓↓	↓↓↓	↓	↑↑↑	↑↑	↑
0.9 U (5 d)	↑↑	-	-	-	-	-	↓↓↓	↑↑↑	↑↑↑	↑↑	↓↓↓	↓↓↓	↓	↑↑↑	↑↑	↑
0.9 U (7 d)	↑↑	-	-	-	-	-	↓↓↓	↑↑↑	↑↑↑	↑↑	↓↓↓	↓↓↓	↓	↑↑↑	↑↑	↑

Note: MB: midbrain, UP: upper pons, LP: lower pons. Addition of a blue arrow (↑) indicates a comparative significant increase, and that of a red arrow (↓) represents a comparative significant decrease from the group of immediate lesser severity in the same time interval. A blacked-out cell indicates no significant difference from controls ($p>0.05$). A dash (-) indicates absence of nystagmus. *Significant difference with saline control only

nick end labeling (TUNEL) assay to measure apoptosis, according to the manufacturer's instructions (TUNEL cell apoptosis detection kit, Nanjing KeyGen Biotech. Co., Ltd.). Ten random fields of each segments (OMN, PPRN and VN) were captured under a high power lens ($\times 200$). Cells with dark-brown nucleoli or nuclear karyorrhexis in the cytoplasm were deemed apoptotic. The percentage of apoptotic cells was calculated as $100\% \times \frac{\text{number of positive cells}}{\text{number of positive cells} + \text{number of negative cells}}$.

Statistical analysis

Continuous data are presented as means \pm standard deviation (SD), and were analyzed by using one-way ANOVA, with the Tukey's post hoc test. Pearson's correlation analysis was used to assess the relations of ICP, NMDAR expression, apoptosis and MBP expression in different parts of the brain. In order to determine the diagnostic accuracy of ENG monitoring of the cold caloric reflex test in localizing brainstem injury, discriminant function analysis

of all ENG parameters (Lat, Freq, Amp, SPV, and CVI) was also performed. Statistical analysis was performed using SPSS16.0 for Windows (SPSS Inc., Chicago, IL, USA). Two-tailed P -values <0.05 were considered statistically significant.

Results

Brainstem sections

Approximately 10% of animals died in group of 0.9 U ICH within 72 h post-surgical procedure. 92% of the 0.9 U ICH animals ($n=48$) were verified with subfalcial herniation approximately during autopsy examination (**Figure 1G**). Representative sections of basal ganglia were shown (coronal sections through the needle track cut 7.0 mm from the frontal pole) from rats sacrificed at 12 h, 24 h, 48 h, 72 h, 5 d and 7 d post-injection (**Figure 1A-H**). No hematomas were visible in the saline control group (**Figure 1B**). Homogenous hematomas that obscured the gray matter boundary were observed in all ICH groups (**Figure 1C, 1E** and

Brainstem injury of cold caloric reflex test

Table 3. ICP of experimental basal ganglia intracerebral hemorrhage induced by variable doses collagenase in rats

Group	n	ICP (mmHg)					
		12 h	24 h	48 h	72 h	5 d	7 d
Sham	3	9.40±0.55 ^{fh}	9.63±0.63 ^{dffh}	9.26±0.32 ^{dffh}	9.66±0.47 ^{dffh}	9.4±0.55 ^{fh}	9.63±0.63 ^{fh}
Saline	8	8.96±0.48 ^{fh}	9.11±0.33 ^{dffh}	9.21±0.62 ^{dffh}	9.16±0.60 ^{dffh}	8.96±0.48 ^{fh}	9.11±0.34 ^{fh}
0.3 U	8	9.61±0.23 ^{fh}	12.61±0.40 ^{bffh}	15.61±0.41 ^{bffh}	13.32±0.98 ^{bffh}	9.63±0.45 ^{fh}	8.96±0.69 ^{fh}
0.6 U	8	12.06±0.44 ^{bdfh}	15.08±0.24 ^{bdfh}	18.35±0.60 ^{bdfh}	18.6±0.37 ^{bdfh}	14.4±0.54 ^{bdfh}	10.57±0.48 ^{bdfh}
0.9 U	8	14.17±2.35 ^{bdf}	20.6±0.50 ^{bdf}	24.67±0.4 ^{bdf}	25.2±0.43 ^{bdf}	18.7±0.40 ^{bdf}	13.53±0.56 ^{bdf}

Note: Compared with control groups (a: $P<0.05$, b: $P<0.01$). Compared with 0.3 U group (c: $P<0.05$, d: $P<0.01$). Compared with 0.6 U group (e: $P<0.05$, f: $P<0.01$). Compared with 0.9 U group (g: $P<0.05$, h: $P<0.01$).

Table 4. ENG parameters induced by the cold caloric test in Rosenberg's ICH model

Group	ENG Parameter	12 h	24 h	48 h	72 h	5 d	7 d
Sham	Lat (s)	26.25±11.83 ^{cd}	26.12±15.71 ^{bcd}	24.86±11.09 ^{bcd}	22.67±11.5 ^{bcd}	26.12±15.71 ^{bcd}	24.88±11.09 ^{cd}
Control	Freq (Hz)	2.95±0.41 ^{cd}	2.55±0.36 ^{bcd}	2.92±0.39 ^{bcd}	2.96±0.39 ^{bcd}	2.92±0.39 ^{bcd}	2.55±0.36 ^{cd}
	Amp (µV)	1.71±0.23 ^{cd}	1.85±0.23 ^{bcd}	1.74±0.21 ^{bcd}	18.01±6.33 ^{bcd}	17.93±5.39 ^{bcd}	14.95±3.67 ^{cd}
	SPV (µV/s)	6.07±0.79 ^{cd}	5.59±1.69 ^{bcd}	6.05±0.76 ^{bcd}	5.97±0.47 ^{bcd}	6.04±0.76 ^{bcd}	5.97±0.42 ^{cd}
	CVI	0.08±0.01 ^{cd}	0.09±0.01 ^{bcd}	0.09±0.00 ^{bcd}	0.08±0.02 ^{bcd}	0.08±0.01 ^{bcd}	0.09±0.04 ^{cd}
Saline	Lat	23.67±8.50 ^{bcd}	22.67±11.50 ^{bcd}	33.33±4.72 ^{bcd}	26.12±15.71 ^{bcd}	33.37±4.73 ^{bcd}	22.67±11.50 ^{cd}
Control	Freq	2.75±0.63 ^{cd}	3.43±0.48 ^{bcd}	2.83±0.53 ^{bcd}	2.83±0.35 ^{bcd}	2.79±0.53 ^{bcd}	2.77±0.48 ^{cd}
	Amp	1.83±0.13 ^{cd}	1.74±0.34 ^{bcd}	1.83±0.06 ^{bcd}	2.28±0.46 ^{bcd}	2.27±0.39 ^{bcd}	2.31±0.44 ^{cd}
	SPV	5.94±0.80 ^{cd}	6.13±0.40 ^{bcd}	5.87±0.84 ^{bcd}	5.80±0.52 ^{bcd}	5.87±0.84 ^{bcd}	5.83±0.48 ^{cd}
	CVI	0.08±0.00 ^{cd}	0.08±0.01 ^{bcd}	0.09±0.01 ^{bcd}	0.08±0.02 ^{bcd}	0.08±0.00 ^{bcd}	0.09±0.00 ^{cd}
0.3 U	Lat	29.25±13.14 ^{acd}	58.25±5.20 ^{bcd}	64.75±2.49 ^{acd}	65.5±2.45 ^{acd}	55.50±3.38 ^{acd}	26.75±15.6 ^{cd}
ICH	Freq	2.91±0.64 ^{cd}	1.48±0.324 ^{acd}	0.73±0.17 ^{acd}	0.66±0.14 ^{acd}	1.77±0.33 ^{acd}	2.84±0.29 ^{cd}
	Amp	1.80±0.43 ^{cd}	1.44±0.33 ^{acd}	1.35±0.25 ^{acd}	1.31±0.24 ^{acd}	1.74±0.25 ^{acd}	1.96±0.29 ^{cd}
	SPV	5.29±1.95 ^{cd}	2.72±0.97 ^{acd}	1.03±0.37 ^{acd}	0.93±0.56 ^{acd}	3.14±0.39 ^{acd}	5.90±1.02 ^{cd}
	CVI	0.08±0.015 ^{cd}	0.26±0.05 ^{acd}	0.37±0.03 ^{acd}	0.46±0.04 ^{acd}	0.26±0.03 ^{acd}	0.08±0.01 ^{cd}
0.6 U	Lat	59.5±7.19 ^{abd}	60.75±5.28 ^{abd}	74.50±10.91 ^{abd}	84.5±6.63 ^{abd}	64.38±3.58 ^{abd}	57.12±3.44 ^{abd}
ICH	Freq	1.66±0.35 ^{abd}	6.91±0.35 ^{abd}	0.21±0.05 ^{abd}	0.19±0.05 ^{abd}	0.39±0.87 ^{abd}	0.95±0.33 ^{abd}
	Amp	1.32±0.30 ^{abd}	1.16±0.22 ^{abd}	1.08±0.27 ^{abd}	0.71±0.23 ^{abd}	1.83±0.06 ^{abd}	1.25±0.42 ^{abd}
	SPV	2.22±0.54 ^{abd}	0.55±0.09 ^{abd}	0.45±0.20 ^{abd}	0.14±0.07 ^{abd}	0.35±0.16 ^{abd}	1.22±0.48 ^{abd}
	CVI	0.27±0.05 ^{abd}	0.42±0.04 ^{abd}	0.64±0.04 ^{abd}	0.79±0.02 ^{abd}	0.45±0.04 ^{abd}	0.25±0.03 ^{abd}
0.9 U	Lat	79.62±5.55 ^{abc}	89.25±6.45 ^{abc}	107.12±15.68 ^{abc}	-	-	-
ICH	Freq	0.23±0.41 ^{abc}	0.08±0.03 ^{abc}	0.05±0.02 ^{abc}	-	-	-
	Amp	0.67±0.15 ^{abc}	0.44±0.21 ^{abc}	0.1±0.00 ^{abc}	-	-	-
	SPV	0.16±0.09 ^{abc}	0.04±0.15 ^{abc}	0.30±0.00 ^{abc}	-	-	-
	CVI	0.35±0.0.04 ^{abc}	0.55±0.04 ^{abc}	0.80±0.26 ^{abc}	-	-	-

Note: All results are presented as means ± SD. Across all ENG parameters, there were significant differences between the 0.6 U ICH, 0.9 U ICH, and the two control groups at all time intervals. There were significant differences between the 0.3 U ICH group and the two control groups at 24 h, 48 h, 72 h, and 5 d. (a) indicates a significant difference with one or both control groups ($p<0.01$), (b) indicates a significant difference with the 0.3 U ICH group ($p<0.01$), (c) indicates a significant difference with the 0.6 U ICH group ($p<0.01$), (d) indicates a significant difference with the 0.9 U ICH group ($p<0.01$), and (-) indicates nystagmus was not induced by the cold caloric test.

1G). The maximum volume of hematoma was shown at 24 h-48 h, and was gradually absorbed after 72 h (**Figure 1C-H**). Midline shift could be seen in the 0.9 U ICH group at 24 h, 48 h, and 72 h (**Figure 1G**).

ICP monitoring

There was no significant difference in ICP (8-10 mmHg, $P>0.05$) between the saline control

group and the sham control group across all time intervals (**Tables 2 and 3**). At 12 h, 5 d, and 7 d, ICP levels of the 0.3 U ICH group were similar to that of saline and sham control groups (all $P>0.05$); at 24 h, 48 h, and 72 h, ICP levels of the 0.3 U ICH group were elevated compared with that in controls ($P<0.01$) (**Tables 2 and 3**). ICP levels in 0.6 U and 0.9 U ICH groups were elevated compared with that in control and the 0.3 U groups at each time point ($P<0.01$)

Brainstem injury of cold caloric reflex test

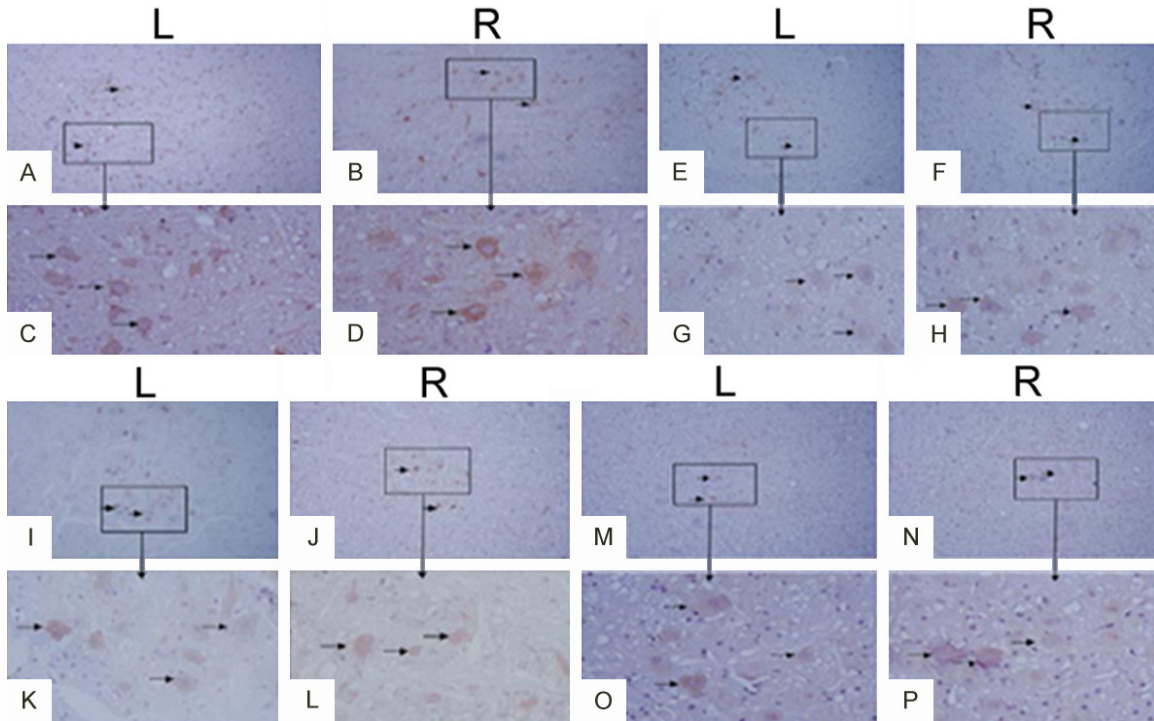


Figure 2. NMDAR1 immunohistochemical staining of the midbrain's OMN with Rosenberg's ICH model. (L: left OMN, R: right OMN, top panel: $\times 100$, bottom panel: $\times 400$). (A-D) the saline control group at 72 h, (E-H) the 0.3 U ICH group at 72 h, (I-L) the 0.6 U ICH group at 72 h, and (M-P) the 0.9 U ICH group at 72 h. All arrows pointed to NMDAR1 + cells; the cell membranes stained brown-yellow, and the nuclei stained blue. The NMDAR1 expression levels were significantly lower in all ICH groups compared with controls. There was an inverse relationship between the dosage of collagenase injected and the level of NMDAR1 expression.

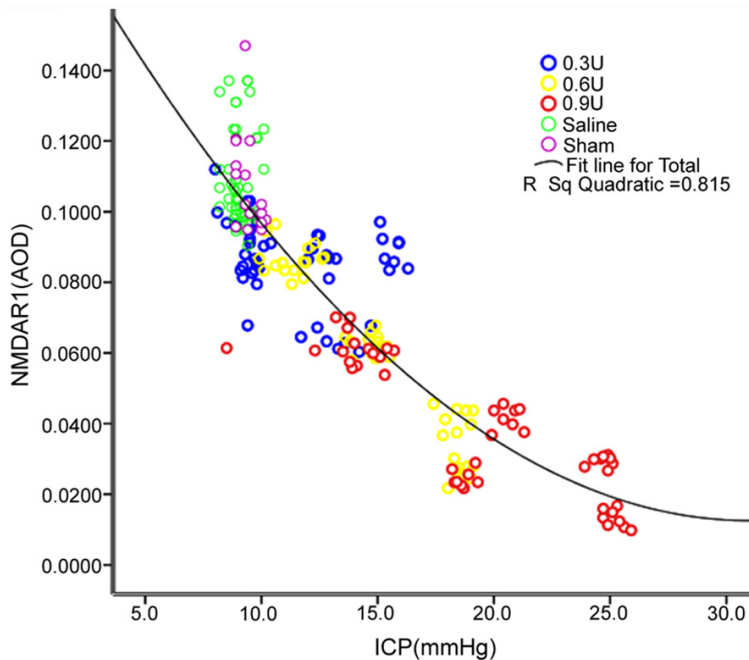


Figure 3. Correlation between ICP levels and AOD of NMDAR1 in the midbrain's OMN. There was a significantly negative correlation between ICP levels and AOD of NMDAR1 in the midbrain's OMN ($r=0.794$, $P<0.01$).

(**Tables 2 and 3**). There were significant differences among the three ICH groups at each time point ($P<0.01$) (**Tables 2 and 3**).

ENG recording of the cold caloric reflex test

All five parameters of ENG were similar ($P>0.01$) between the two control groups at all time points (**Tables 2 and 4**). At 12 h, the Lat of the 0.3 U ICH group was significantly longer than that of controls ($P<0.01$); all other ENG parameters in the 0.3 U ICH group at 12 h showed similar with controls ($P>0.05$, **Tables 2 and 4**). In the 0.3 U ICH group, no significant difference in all ENG parameters was observed compared to controls at day 7 ($P>0.05$, **Tables 2 and 4**).

Brainstem injury of cold caloric reflex test

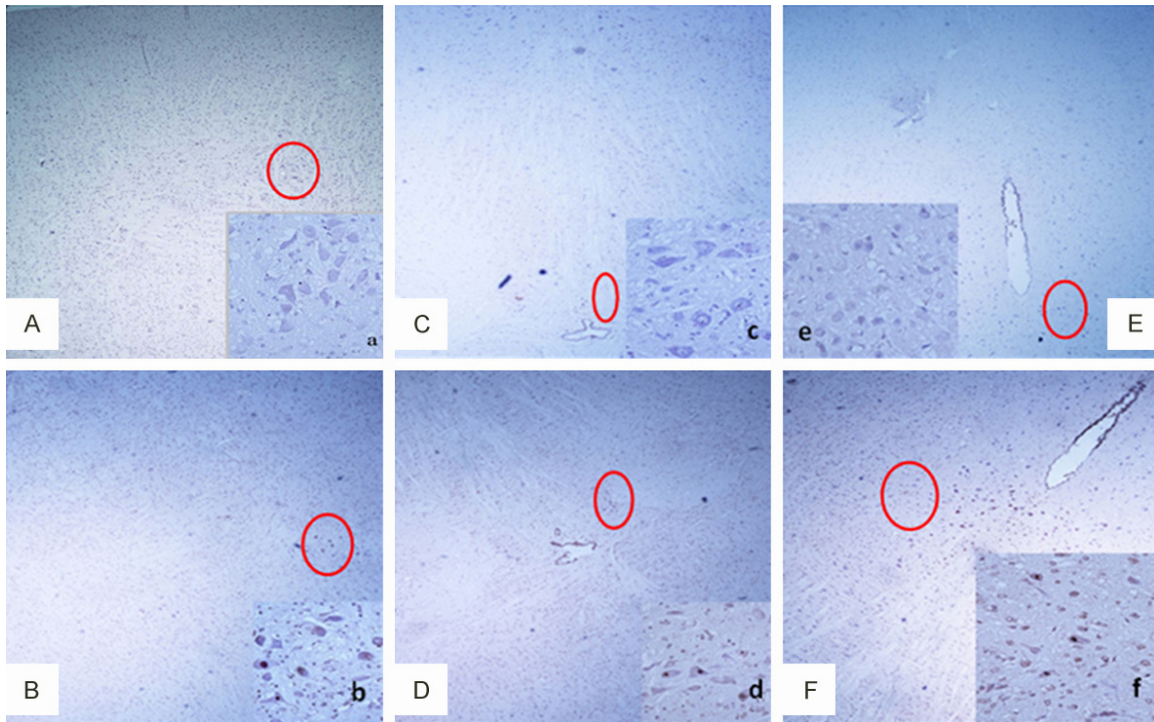


Figure 4. Apoptotic TUNEL assay of various brainstem segments of Rosenberg's ICH model. A and B: Showed the normal and abnormal midbrain ($\times 40$). C and D: Showed the normal and abnormal upper pons, respectively ($\times 40$). E and F: Showed the normal and abnormal lower pons, respectively ($\times 40$). The insets (a-f) magnified the structures within the red circle ($\times 400$). TUNEL assay of apoptotic cells showed dark-brown nucleoli, nuclear karyorrhexis, and dark-brown particulates in the cytoplasm.

However, in the 0.6 U and 0.9 U ICH groups, the Lat and CVI were significantly increased, and the Freq, Amp, and SPV were decreased compared with controls ($P < 0.01$, **Tables 2 and 4**). All ENG parameters in the 0.6 U ICH group were statistically different from controls through day 7 ($P < 0.01$, **Tables 2 and 4**). Nystagmus induced in the 0.9 U ICH group showed a decreasing trend of ENG level after surgery. The nystagmus stopped completely after 72 h and remained inactive till day 7 (**Tables 2 and 4**).

Correlations between ICP and ENG parameters

There were positive correlations between ICP and Lat ($r = 0.623$, $P < 0.01$) and CVI ($r = 0.846$, $P < 0.01$), and negative correlations between ICP and SPV ($r = -0.766$, $P < 0.01$), Amp ($r = -0.782$, $P < 0.01$), and Freq ($r = -0.804$, $P < 0.01$). ([Supplementary Figure 5](#)).

NMDAR1 & GABA-A α 1 expression in OMN

The average optical density (AOD) of both NMDAR1 and GABA-AR α 1 were bilaterally symmetric ($P > 0.05$) at all time points in both con-

trol groups. There was no significant difference in the AOD of NMDAR1 and GABA-AR α 1 between the two control groups at each time point ($P > 0.05$) (**Table 2**).

AOD of NMDAR1 was reduced in all three ICH groups compared with controls groups ($P < 0.01$, **Figure 2**). Moreover, there was significant difference among all three ICH groups ($P < 0.01$) (**Table 2, Figure 2**). There was a negative collagenase dose-dependent relationship with the AOD of NMDAR1 ($P < 0.05$) (**Table 2**). Pearson correlation analysis demonstrated a negative correlation between ICP levels and NMDAR1 expression in the OMN in a negative collagenase dose-dependent manner ($P < 0.05$, **Figure 3; Table 2**). There was no significant difference in the AOD of GABA-AR α 1 between the three ICH groups and controls ($P > 0.05$).

Apoptosis

At all time points, there was no significant difference in apoptotic cell levels between the two control groups ($P > 0.05$, **Figure 4; Table 2**).

Brainstem injury of cold caloric reflex test

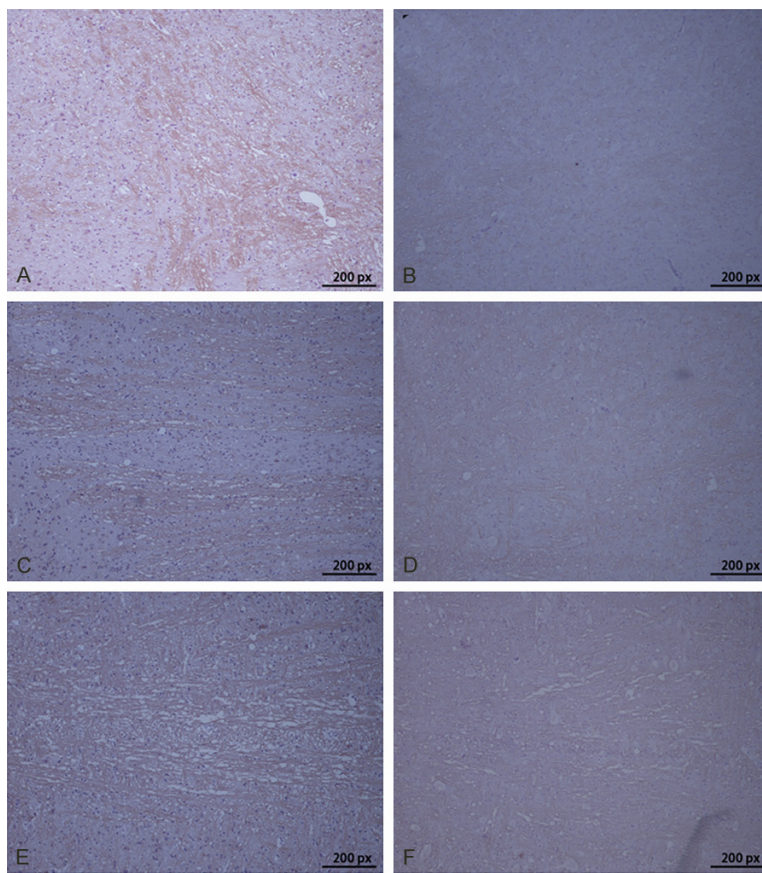


Figure 5. MBP immunohistochemical staining of various brainstem segments of Rosenberg's ICH model. A and B: Showed the normal and abnormal midbrain, respectively ($\times 100$). C and D: Showed the normal and abnormal upper pons, respectively ($\times 100$). E and F: Showed the normal and abnormal lower pons, respectively ($\times 100$). Abnormal MBP staining showed weak myelin staining accompanied by a disrupted bundle structure.

However, the apoptotic cell levels of all three ICH groups were higher than those of controls in the midbrain and upper pons ($P < 0.01$). In all ICH groups, the amount of apoptotic cells was significantly increased in the midbrain at 12 h and thereafter, while the percentage of apoptotic cells grew significantly across both the midbrain and upper pons at 48 h and thereafter ($P < 0.01$, **Figure 4; Table 2**). Moreover, in the 0.6 U and 0.9 U ICH groups, the numbers of apoptotic cells in the lower pons elevated at 48 h and thereafter ($P < 0.01$, **Figure 4; Table 2**). However, in the 0.3 U ICH group, the amount of apoptotic cells was not different from controls in the lower pons. The apoptotic cells increased in a collagenase dose-dependent manner ($P < 0.05$, **Figure 4; Table 2**).

MBP expression in the MLF

In a portion of the ICH subgroups, high magnification ($\times 400$) of the MLF revealed demyelination

through weakened myelin staining and a disrupted bundle structure (**Figure 5**). In the control groups, the MLF were in an ordered bundled structure. There were no significant differences in the AOD of MBP between the control groups ($P > 0.05$). The AOD of MBP in the midbrain first showed a significant decline at 12 h, 24 h, and 72 h in the 0.9 U, 0.6 U, and 0.3 U ICH groups, respectively (**Table 2**). The AOD of MBP in the upper pons first exhibited a significant decline at 48 h and 72 h in the 0.9 U and 0.6 U ICH groups, respectively (**Table 2**). Only the 0.9 U ICH group displayed a significantly abnormal expression of MBP extending to the lower pons, showing an initially significant decline at 48 h ($P < 0.05$, **Table 2**). There was a negative correlation between collagenase and observable demyelination, the AOD of MBP ($P < 0.05$, **Figure 5; Table 2**).

Discriminant analysis of ENG parameters

The calculation was derived from multiple discriminant analysis (MDA) function, which identified the relationship among multiple variables and predicted the likelihood of an observed parameter affiliated to the classified pattern. The result of the MDA analysis suggested that the prediction reached the accuracy of 79.5% for the specific region of brainstem damage (**Figure 6, Supplementary Figures 3 and 4**).

Discussion

In the observation of brainstem injury associated with supratentorial lesions, increasing lesion severity was indicated to be correlated with higher ICP and with higher levels and rostral-caudal progression of electronystagmographic abnormalities, neuronal apoptosis, demyelination, and NMDAR1 down-regulation. Analysis of ENG parameters showed a 79.5% of diagnostic accuracy in localizing brainstem injury.

Brainstem injury of cold caloric reflex test

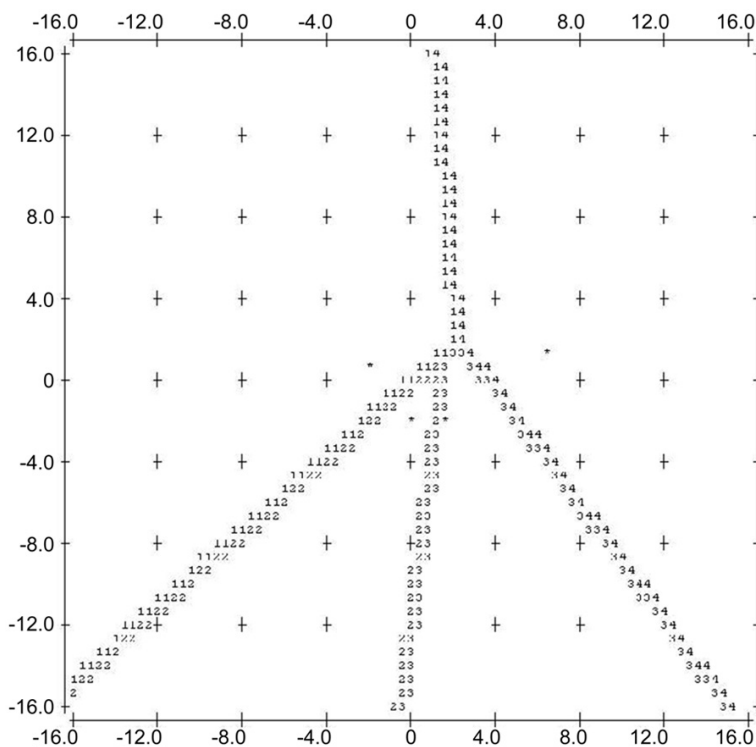


Figure 6. Territorial map of the discriminant function analysis of ENG parameters recorded with the cold caloric reflex test. Territorial mapping of the discriminant analysis showed that data clusters corresponding to the different regions of the brainstem function injury (1: normal brainstem, 2: midbrain injury, 3: superior pons injury, 4: inferior pons injury) can be visually discriminated from each other. Most of individuals with normal brainstem function were located in the 1/3 left upper quadrant, the individuals with midbrain injury and superior pons injury were located in the 1/3 left and right of the lower quadrant relatively. Individuals with inferior pons injury were located in the right the upper quadrant.

By means of Rosenberg's ICH model [6, 7], we established supratentorial lesions of varying severity in vivo. Consequently, varying degrees of ICP elevation and VOR hyporeflexia were measured. Our data showed that ICP was related to the extent of brain injury. Increasing lesion severity was correlated with a significantly higher ICP elevation, longer nystagmus latency, shorter nystagmus frequency, smaller nystagmus amplitude, slower nystagmus SPV, higher nystagmus CVI, and a more irregular nystagmus rhythm. The most serious outcome was the complete VOR areflexia, which occurred in the 0.9 U ICH group at 72 h and lasted throughout the study period (day 7). These results indicated that the severity of the initial supratentorial lesion differentially affected both ICP levels and ENG parameters. In addition, Pearson correlation analysis demonstrated that changes in ICP levels were correlated with changes across all five ENG parameters.

As the progression of ENG parameters and staining abnormalities showed that brainstem injury proceeded rostral-caudally from the midbrain to the lower pons in correlation with increasing ICP levels and lesion severity, our research firstly suggested that ICP elevation was involved in brainstem injury associated with supratentorial lesions. Inao et al [1] have already detailed the anatomical changes of brainstem displacement in the setting of supratentorial lesions via imaging. However, the imaging was not performed in the present study. Macroscopic pathological changes similar to those caused by brainstem displacement were confirmed by the anatomical progression of ENG parameter abnormalities. In addition, histopathological changes such as neuronal apoptosis, demyelination, NMDAR1 under-expression and abnormal HE staining were also observed in the ICH groups. Specifically, we found that in line with increasing lesion severity and ICP elevation,

midbrain injury occurred first, followed by the injury in the upper pons and then the lower pons. The damage in lower pons was consistently accompanied by midbrain lesions, and upper pons injury by more severe lesions. However, several cases of lower severity injury occurred solely in the midbrain and upper pons, leaving the lower pons unmarred.

As stated above, even if ICP was associated with the level of the lesion, ICP was not correlated to histopathological changes. In addition, we cannot exclude the possibility that the collagenase induced some histopathological changes that could have occluded the changes induced by ICP. Nevertheless, it can be reasonably surmised that the sequence of damage proceeded rostral-caudally from the midbrain to the lower pons with increasing lesion severity.

Brainstem injury of cold caloric reflex test

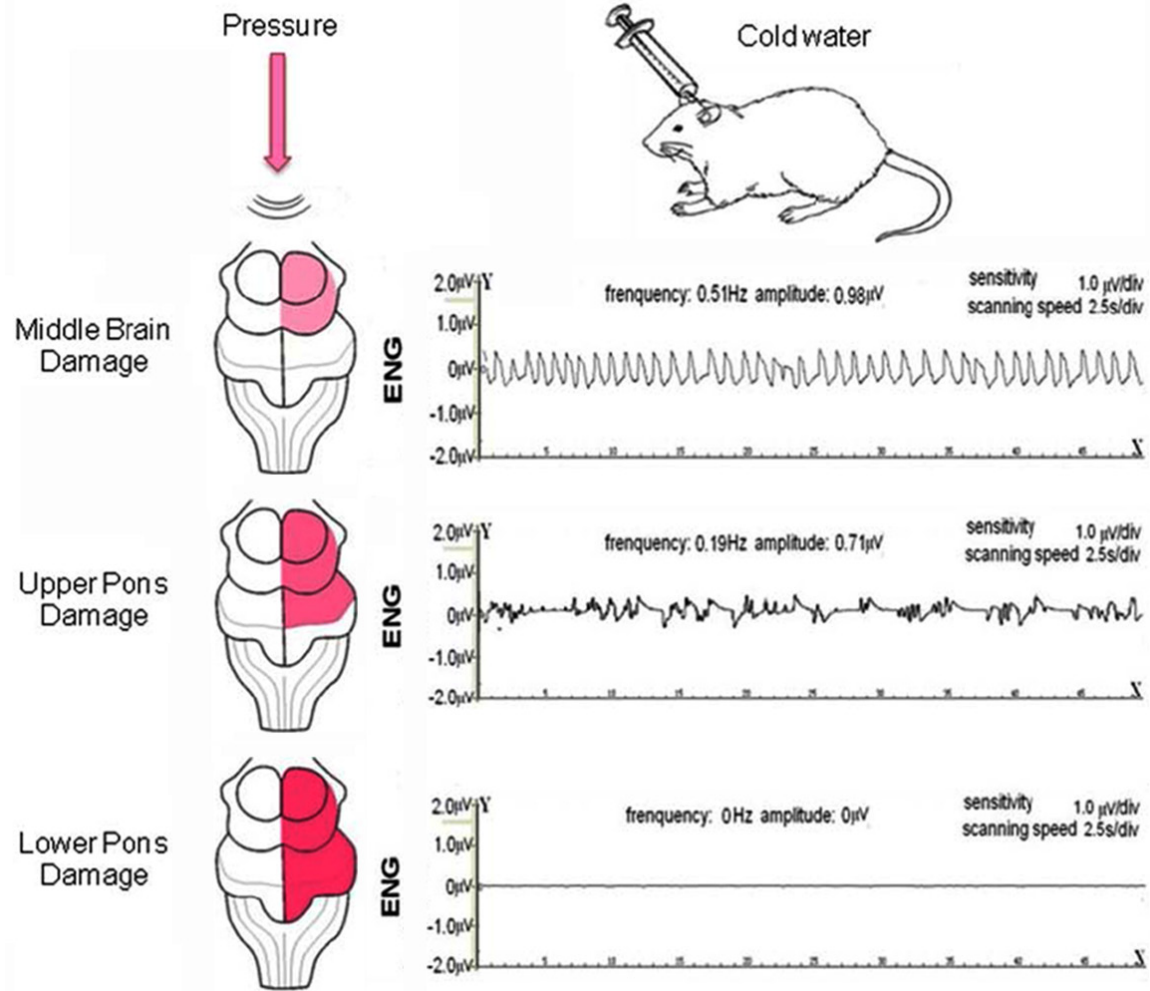


Figure 7. Localization of brainstem injury via ENG monitoring. Representative ENG traces corresponding to the healthy control groups were detected at various regions of brainstem injury derived from the three ICH groups (all recorded at 72 h). Consistent with the findings from the discriminant function analysis of the ENG parameters, all traces can be visually discriminated from one another. (Middle Brain Damage, Upper Pons Damage, Lower Pons Damage).

Interestingly, abnormal values of ENG parameters, increased neuronal apoptosis, and decreased NMDAR1 expression were observed in the 0.3 U ICH group at 24 h and in the 0.6 U ICH group at 12 h, but the corresponding myelination and HE findings of these groups were normal. Thus, abnormal ENG read-outs produced in the context of supratentorial lesions cannot be solely attributed to demyelination and/or histopathologic changes. These small-scale phenomena were insufficient for the detection through modern imaging methods.

Cold caloric reflex is a one of brainstem reflexes which is usually used to identify brain death [25]. As a type of VOR (vestibular ocular reflex),

its anatomy loop crosses over from the rostral to caudal of the brainstem. Accidental links of the loop may result in the abnormality of VOR. The feasibility of the foregoing ENG monitoring technique as a diagnostic method for localizing brainstem injury was evaluated in the present study. All subjects were categorized according to different segments of brainstem damage, and then assigned numerical values derived from their respective ENG parameters. The discriminant function analysis of this data showed a 79.5% accuracy rate in localizing brainstem injury. Territorial mapping there revealed that data clusters corresponding to different levels of the brainstem can be visually discriminated from one another, indicating ENG a potential

Brainstem injury of cold caloric reflex test

tool to predict the progress of supratentorial lesions (as suggested in **Figure 7**). ENG is a complimentary test on top of ICP to estimate the function of brainstem after supratentorial lesions. Cold caloric test with ENG predicted the changes of brainstem function directly which ICP may not show. Additionally, ENG quantitatively detected the functional changes of the lesion located in midbrain, superior pons and inferior pons based the VOR anatomical loop. Also ENG is far less invasive and easily operated method. This convenient bedside diagnostic method with a relatively high accuracy rate of lesion localization provided a valuable tool for clinical practitioners in the diagnosis, prognosis and treatment of brainstem injury.

However, the main limitation of the present study still exists that it was conducted with a rat model. Indeed, the structure of rat brain is different from that of humans. In addition, the lesions caused by ICP in the rat brain might show discrepancy from that in the human brain. Therefore, further clinical trials on patients are required for the validation of this method.

In conclusion, our study showed a possible ICP involvement in brainstem injury in the setting of supratentorial lesions using the Rosenberg's ICH model in rats. Moreover, the high accuracy rate of lesion localization shows that the cold caloric reflex test for ENG monitoring may be an effective diagnostic tool in localizing brainstem injury at the bedside.

Acknowledgements

This work was supported by National basic research program of China (973 program, No: 2009CB183000).

Disclosure of conflict of interest

None.

Address correspondence to: Dr. Peng Xie, Department of Neurology, The First Affiliated Hospital of Chongqing Medical University, Chongqing 400016, China. Tel: +86-021-64085875; Fax: +86-021-64085875; E-mail: pengxiedfg@163.com

References

[1] Inao S, Kuchiwaki H, Kanaiwa H, Sugito K, Banno M and Furuse M. Magnetic resonance

imaging assessment of brainstem distortion associated with a supratentorial mass. *J Neurol Neurosurg Psychiatry* 1993; 56: 280-285.

- [2] Howell DA. Longitudinal brain stem compression with buckling. Some further observations on a form of upper brain stem compression with intracranial space occupying lesions and brain swelling. *Arch Neurol* 1961; 4: 572-579.
- [3] Wijdicks EF and Miller GM. MR imaging of progressive downward herniation of the diencephalon. *Neurology* 1997; 48: 1456-1459.
- [4] Stone JL, Ghaly RF, Subramanian KS, Roccaforte P and Kane J. Transtentorial brain herniation in the monkey: analysis of brain stem auditory and somatosensory evoked potentials. *Neurosurgery* 1990; 26: 26-31.
- [5] Wijdicks EF. Acute brainstem displacement without uncal herniation and posterior cerebral artery injury. *BMJ Case Rep* 2009; 2009: bcr2007126227.
- [6] Pfefferkorn T and Rosenberg GA. Closure of the blood-brain barrier by matrix metalloproteinase inhibition reduces rtPA-mediated mortality in cerebral ischemia with delayed reperfusion. *Stroke* 2003; 34: 2025-2030.
- [7] Rosenberg GA, Mun-Bryce S, Wesley M and Kornfeld M. Collagenase-induced intracerebral hemorrhage in rats. *Stroke* 1990; 21: 801-807.
- [8] Han SG, Kim GM, Lee KH, Chung CS and Jung KY. Reflex movements in patients with brain death: a prospective study in a tertiary medical center. *J Korean Med Sci* 2006; 21: 588-590.
- [9] Watts J. Brain-death guidelines revised in Japan. *Lancet* 1999; 354: 1011.
- [10] Wijdicks EF, Varelas PN, Gronseth GS, Greer DM; American Academy of Neurology. Evidence-based guideline update: determining brain death in adults: report of the Quality Standards Subcommittee of the American Academy of Neurology. *Neurology* 2010; 74: 1911-1918.
- [11] Baba S, Fukumoto A, Aoyagi M, Koizumi Y, Ikezono T and Yagi T. A comparative study on the observation of spontaneous nystagmus with Frenzel glasses and an infrared CCD camera. *J Nippon Med Sch* 2004; 71: 25-29.
- [12] Batuecas-Caletrio A, Montes-Jovellar L, Boleas-Aguirre MS and Perez-Fernandez N. The ice-water caloric test. *Acta Otolaryngol* 2009; 129: 1414-1419.
- [13] Mohamed ES, Kaf WA, Rageh TA, Kamel NF and Elattar AM. Evaluation of patients with vertigo of vertebrobasilar insufficiency origin using auditory brainstem response, electronystagmography, and transcranial Doppler. *Int J Audiol* 2012; 51: 379-388.

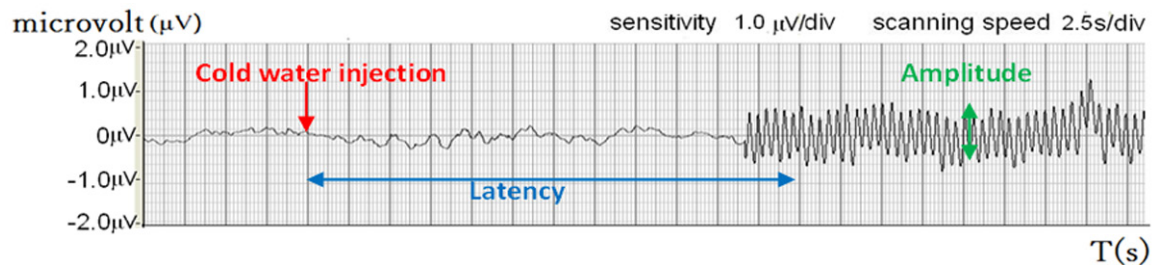
Brainstem injury of cold caloric reflex test

- [14] Goncalves DU, Felipe L and Lima TM. Interpretation and use of caloric testing. *Braz J Otorhinolaryngol* 2008; 74: 440-446.
- [15] Marx JJ, Mika-Gruettner A, Thoemke F, Fitzek S, Fitzek C, Vucurevic G, Urban PP, Stoeter P and Hopf HC. Electrophysiological brainstem testing in the diagnosis of reversible brainstem ischemia. *J Neurol* 2002; 249: 1041-1047.
- [16] Yagi T. Nystagmus as a sign of labyrinthine disorders—three-dimensional analysis of nystagmus. *Clin Exp Otorhinolaryngol* 2008; 1: 63-74.
- [17] Yagi T, Koizumi Y, Aoyagi M, Kimura M and Sugizaki K. Three-dimensional analysis of eye movements using four times high-speed video camera. *Auris Nasus Larynx* 2005; 32: 107-112.
- [18] Struijk JJ, Kanters JK, Andersen MP, Hardahl T, Graff C, Christiansen M and Toft E. Classification of the long-QT syndrome based on discriminant analysis of T-wave morphology. *Med Biol Eng Comput* 2006; 44: 543-549.
- [19] Kaaber EG and Zilstorff K. Vestibular function in benign intracranial hypertension. *Clin Otolaryngol Allied Sci* 1978; 3: 183-188.
- [20] Rosenberg M, Sharpe J and Hoyt WF. Absent vestibulo-ocular reflexes and acute supratentorial lesions. *J Neurol Neurosurg Psychiatry* 1975; 38: 6-10.
- [21] Kuo TB and Yang CC. Frequency domain analysis of electrooculogram and its correlation with cardiac sympathetic function. *Exp Neurol* 2009; 217: 38-45.
- [22] Todorova MG, Turksever C, Schotzau A, Schorderet DF and Valmaggia C. Metabolic and functional changes in retinitis pigmentosa: comparing retinal vessel oximetry to full-field electroretinography, electrooculogram and multifocal electroretinography. *Acta Ophthalmol* 2016; 94: e231-241.
- [23] Mulch G, Leonardy B and Petermann W. Which are the parameters of choice from the evaluation of caloric nystagmus? *Arch Otorhinolaryngol* 1978; 221: 23-35.
- [24] Covenas R, Gonzalez-Fuentes J, Rivas-Infante E, Lagartos-Donate MJ, Mangas A, Geffard M, Arroyo-Jimenez MM, Cebada-Sanchez S, Insauti R and Marcos P. Developmental study of vitamin C distribution in children's brainstems by immunohistochemistry. *Ann Anat* 2015; 201: 65-78.
- [25] Wijdicks EF. The diagnosis of brain death. *N Engl J Med* 2001; 344: 1215-1221.

Brainstem injury of cold caloric reflex test



Supplementary Figure 1. The positions of electrodes to record the ENG with cold caloric reflex in rat. The RM6240C multi-channel polygraph recorder records the eye movement wave through potential differences produced by the eye movements at horizontal and vertical positions. Prior to ENG measurement, reference electrode was implanted subcutaneously in the center of the animal's forehead while two recording electrodes were implanted in angulus oculi lateralis (lateral) and angulus oculi nasalis (middle) respectively by each eye of the animal. The positive electrodes were placed in the angulus oculi nasalis of the left eye and the angulus oculi nasalis of the right eye, this resulted a positive wave recorded by the instrument when eyeballs move toward the right. Conversely, the negative electrodes were placed in the angulus oculi nasalis of the right eye and the angulus oculi nasalis of the left eye that resulted a negative wave recorded by the instrument when the eyeball move towards the left. Hence, the waves are recorded as microvolty (μV) instead of degree (eye position).



Supplementary Figure 2. ENG recorded with the cold caloric reflex in normal rat. X-axis represents time measured in second (s) where each square represents 2.5 s. Y-axis represents amplitude of nystagmus measured in microvolt (μV). Cold water was injected (red arrow) to animal after the amplitude of ENG stabilized around $0 \pm 0.25 \mu\text{V}$ for 30 s (not shown). Latency of nystagmus (blue) was the time interval from the start of irrigation to the appearance of continuous nystagmus (defined as >5 sequential waves of identical frequency and amplitude with each constituent wave demonstrating both slow and fast phases). The green arrow segment represented the amplitude of the nystagmus.

Brainstem injury of cold caloric reflex test

$$y_1 = -29.743 + 0.013\text{Lat} + 8.497\text{F} + 11.368\text{Amp} + 1.334\text{SPV} + 59.545\text{CVI}$$

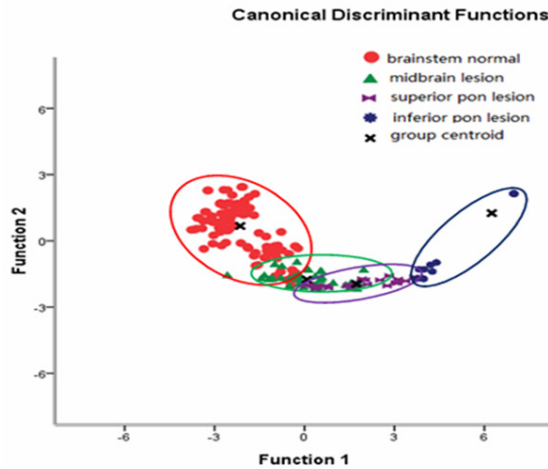
$$y_2 = -23.211 - 0.002\text{Lat} + 6.019\text{F} + 9.516\text{AMP} + 0.615\text{SPV} + 69.005\text{CVI}$$

$$y_3 = -30.95 - 0.020\text{Lat} + 6.224\text{F} + 6.877\text{AMP} + 1.442\text{SPV} + 90.479\text{CVI}$$

$$y_4 = -68.800 + 0.096\text{Lat} + 7.941\text{F} + 2.47\text{AMP} + 3.444\text{SPV} + 115.913\text{CVI}$$

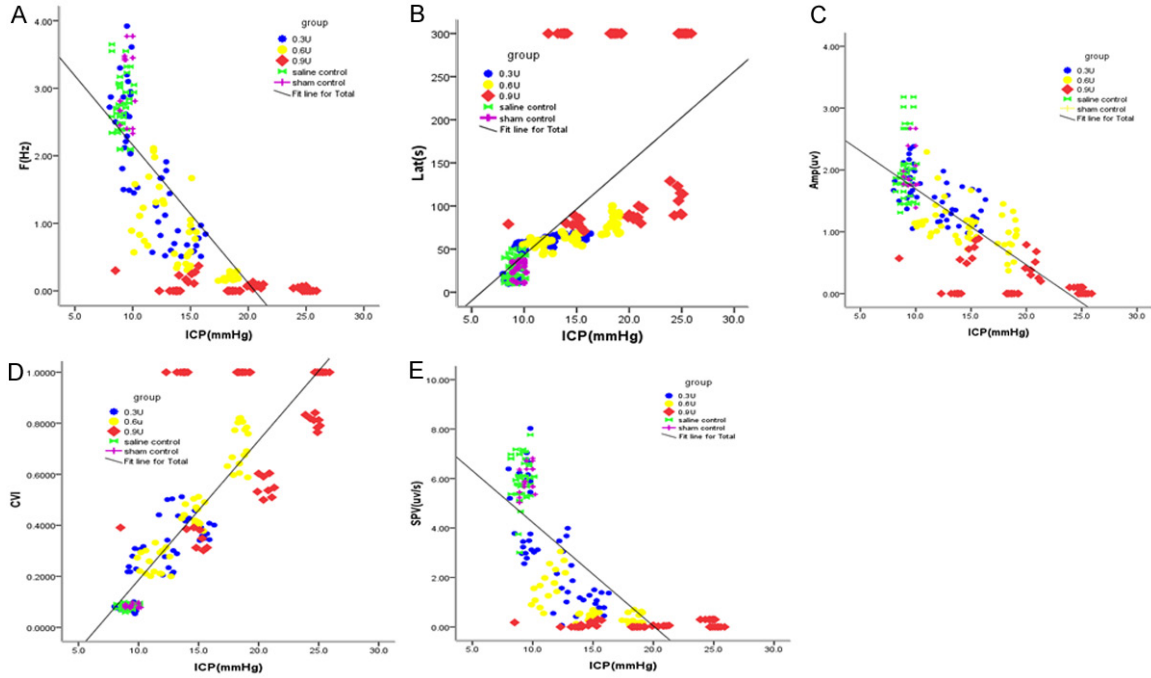
No	representation	ENG parameters	Abbreviation
1	Normal brainstem function	latency	Lat
2	midbrain functional injury	frequency	F
3	superior pons functional injury	amplitude	Amp
4	inferior pons functional injur	slow-phase velocity	SPV
		circadian variation index	CVI

Supplementary Figure 3. Equations between the ENG parameters recorded with the cold caloric reflex test and the brainstem injury after ICH in rats. The equations derived from multiple discrimination analysis (MDA). Four numerical numbers (y_1, y_2, y_3, y_4) could be calculated after the five ENG parameters being measured through the four equations. The biggest one of the four numerical number implied the location of brainstem functional injury. For example, if the biggest one was y_3 so it implied the existence of superior pons functional injury.



Supplementary Figure 4. Territorial map of the discriminant function analysis of ENG parameters recorded with the cold caloric reflex test. The figure was generated based ENG parameters collected from 288 animals. The analysis showed tight cluster of normal brainstem (red). While overlaps were shown in midbrain lesion (green) superior pons lesion (purple) and inferior pons lesion (blue) due to close proximity. According the brainstem pathology of ICH model rats being sacrificed at 72h, the rats were divided into four groups including normal brainstem, midbrain lesion, superior pons lesion, inferior pons lesion. The ENG parameters data with the cold caloric reflex test from all the four groups were discriminated and analyzed for whether there has individual homogeneity within each group and heterogeneity among the four groups. The graph showed there has clear distribution among the four groups.

Brainstem injury of cold caloric reflex test



Supplementary Figure 5. The association between ENG parameters with the cold caloric reflex test and intracranial cerebral pressure (ICP) A: Frequency of ENG decreased along the increased ICP ($r = -0.804$, $P < 0.01$); B: Latency of ENG lengthened along the increased ICP ($r = 0.623$, $P < 0.01$); C: Amplitude of ENG descended along the increased ICP ($r = -0.782$, $P < 0.01$); D: CVI increased along the increased ICP ($r = 0.846$, $P < 0.01$); E: SPV descended along the increased ICP ($r = -0.766$, $P < 0.01$).